Published in final edited form as:
*Dev Cell*. 2011 April 19; 20(4): 526–539. doi:10.1016/j.devcel.2011.02.010.

# Blood vessel tubulogenesis requires Rasip1 regulation of GTPase signaling

**Ke Xu**[1], **Anastasia Sacharidou**[2], **Stephen Fu**[1], **Diana C. Chong**[1], **Brian Skaug**[1,3], **Zhijian J. Chen**[1,3], **George E. Davis**[2], and **Ondine Cleaver**[1,*]

[1] Departments of Molecular Biology, University of Texas Southwestern Medical Center, 5323 Harry Hines Blvd., Dallas, Texas, USA 75390

[2] Department of Medical Pharmacology and Physiology, University of Missouri School of Medicine and Dalton Cardiovascular Research Center, MA 415 Medical Sciences Bldg., Columbia, MO, USA 65212

[3] Howard Hughes Medical Institute, University of Texas Southwestern Medical Center, 5323 Harry Hines Blvd., Dallas, Texas, USA 75390

## SUMMARY

Cardiovascular function depends on patent blood vessel formation by endothelial cells (ECs). However the mechanisms underlying vascular 'tubulogenesis' are only beginning to be unraveled. We show that endothelial tubulogenesis requires the Ras interacting protein 1, Rasip1, and its binding partner the RhoGAP Arhgap29. Mice lacking Rasip1 fail to form patent lumens in all blood vessels, including the early endocardial tube. Rasipl null angioblasts fail to properly localize the polarity determinant Par3 and display defective cell polarity, resulting in mislocalized junctional complexes and loss of adhesion to extracellular matrix (ECM). Similarly, depletion of either Rasip1 or Arhgap29 in cultured ECs blocks *in vitro* lumen formation, fundamentally alters the cytoskeleton and reduces integrin-dependent adhesion to ECM. These defects result from increased RhoA/ROCK/myosin II activity and blockade of Cdc42 and Rac1 signaling. This study identifies Rasip1 as a unique, endothelial-specific regulator of Rho GTPase signaling, which is essential for blood vessel morphogenesis.

## INTRODUCTION

Tubulogenesis is a fundamental process that is essential for the development of many tubular organs, including the cardiovascular system. The first embryonic blood vessels form on embryonic day 8.0 (E8.0) via a process termed *vasculogenesis*. Vasculogenesis is comprised of three principal steps: angioblast (EC progenitor) specification, followed by 'cord' formation, and ultimately blood vessel lumen formation, or 'tubulogenesis'. In the mouse, angioblasts arise within the mesoderm and migrate to adhere with each other in primitive lumenless cords, presaging the paired dorsal aortae, endocardium and yolk sac

[*]Address correspondence to: Ondine Cleaver, Department of Molecular Biology, NA8.300, University of Texas Southwestern Medical Center, 5323 Harry Hines Blvd., Dallas, Texas 75390-9148, USA. Phone: (214) 648-1647;, Fax: (214) 648-1196; ondine.cleaver@utsouthwestern.edu.

SUPPLEMENTAL INFORMATION

Supplemental Information includes Supplemental Experimental Procedures, 7 figures and 6 movies and can be found online at: xxx

vascular plexus. As cords undergo tubulogenesis, ECs create a central lumen, allowing blood flow. The transformation of solid endothelial cords or individual ECs into patent vascular tubes is thus fundamental to establishing a seamless, functional circulatory system and has been the focus of growing interest (Davis et al., 2007; Iruela-Arispe and Davis, 2009; Kamei et al., 2006; Kucera et al., 2007; Strilic et al., 2009).

The precise cellular and molecular mechanistic basis for this morphogenetic process *in vivo* is still not completely understood. While epithelial and endothelial *in vitro* systems have long provided models to dissect mechanisms of lumen formation (Andrew and Ewald; Bayless and Davis, 2002; Davis et al., 2007; Iruela-Arispe and Davis, 2009; Koh et al., 2008; Koh et al., 2009; O'Brien et al., 2002), *in vivo* studies have only begun to elucidate underlying regulatory molecules responsible for vascular tubulogenesis (Kamei et al., 2006; Strilic et al., 2009; Zovein et al.). To date, molecular mechanisms linked to vascular lumen formation have involved either widely expressed regulatory factors, such as Rho family GTPases or integrins (Bayless and Davis, 2002; Connolly et al., 2002; Zovein et al., 2010), or endothelial factors whose ablation hinders lumen formation in only subsets of vessels (Carmeliet et al., 1999), leaving open the question of whether any endothelial-restricted factor might broadly regulate vessel tubulogenesis. Identifying critical endothelial-specific modulators of these pathways has thus represented an important challenge. Understanding, and potentially clinically targeting, the formation and maintenance of vascular lumens is directly relevant to both anti-angiogenic and vascular-targeted therapies (Bergers and Hanahan, 2008; Reardon et al., 2008; Siemann et al., 2005).

Here, we report that blood vessel tube formation requires the endothelial-restricted Ras interacting protein 1, Rasip1. Mice lacking Rasip1 fail to form patent lumens in all blood vessels, large and small, and endocardial development is arrested at the onset of cardiovascular development. We show that Rasip1 acts as a tissue-specific regulator of GTPase signaling, promoting proper establishment of cell polarity, as well as regulating cytoskeletal and cell adhesion changes to drive endothelial tube morphogenesis. Rasip1 regulates activity of Rho GTPases in part by recruiting the RhoA-specific GTPase activating protein (GAP) Arhgap29. Depletion of either Rasip1, or Arhgap29, in cultured ECs aberrantly elevates RhoA/ROCK/Myosin II signaling and blocks Cdc42/Rac1 signaling. As a result, β1 integrin adhesion to ECM is suppressed, the polarity determinant Par3 fails to localize properly, and ectopic tight junctions form at the apical membrane. Our studies identify Rasip1 as a critical and vascular-specific regulator of GTPase signaling, cell architecture and adhesion, which is essential for EC morphogenesis and blood vessel tubulogenesis.

## RESULTS

### Rasip1 is essential for cardiovascular development

To identify genes that regulate blood vessel morphogenesis, we transcriptionally profiled isolated embryonic aortic ECs (Affymetrix, data not shown). Rasip1 (Mitin et al., 2004) was identified as a highly enriched sequence in E8.5 aortic ECs, which was expressed exclusively in ECs of murine, amphibian and fish embryos throughout embryogenesis (Figure 1A–1D) (Xu et al., 2009a). To examine whether Rasip1 might regulate vasculogenesis in higher vertebrates, we generated mice lacking Rasip1 function (Figure S1). Heterozygous *Rasip1* mice were phenotypically normal and viable, while the null mutation was embryonic lethal. Homozygous null embryos appeared grossly normal at E8.25, but were dead by E10.5 (Figure S2A and S2B, and data not shown). At E9.5, *Rasip1*$^{-/-}$ mutant embryos displayed growth retardation and widespread edema (Figure 1E and 1F) and their yolk sac appeared smooth, lacking the hierarchical vascular network

evident in heterozygous controls (Figure 1G and 1H). No significant differences were found in placental tissues (data not shown).

## Blood vessel tubulogenesis requires Rasip1

To understand the origins of the observed cardiovascular failure in *Rasip1*$^{-/-}$ mutants, we sought to characterize developing blood vessels. A Flk1-LacZ allele was bred into the *Rasip1* null line (Shalaby et al., 1995). Initial angioblast numbers and distribution were normal (Figure S2C and S2D), indicating that Rasip1 is not required for angioblast specification, proliferation, or patterning. However by E9.5, mutant vessels failed to remodel from an initial plexus into their typical hierarchical array of large and small vessels, both in the yolk sac (Figure 1I and 1J) and embryonic tissues (Figure 1K and 1L). In addition, arteriovenous differentiation failed in *Rasip1*$^{-/-}$ vessels, as assessed by the arterial marker Connexin40 (Gja5) and EphB4-LacZ (Wang et al., 1998) (Figure 1M-1P). Together, these results showed that development of embryonic blood vessels was severely impaired in the absence of Rasip1.

Remodeling and arteriovenous differentiation defects are hallmark effects of hemodynamic failure, as both processes depend on blood flow (le Noble et al., 2004). Therefore, to identify possible vessel occlusions in *Rasip1* mutants that would hinder blood circulation, we examined the first major embryonic vessels, the paired dorsal aortae. In both *Rasip1*$^{+/-}$ and *Rasip1*$^{-/-}$ embryos, E8.0–8.5 pre-aortal angioblasts aligned normally in two parallel rows, however they appeared distinctly narrower in mutant embryos (Figure S2E–S2L), often displaying visible occlusions (Figure 1Q and 1R). Indeed, sections revealed that patent, continuous lumens were globally absent in all blood vessels, including those of the dorsal aortae (Figure 1S–1V), endocardium (Figure 1W–1X), yolk sac (Figure 1Y–1Z′), vitelline artery, inflow tracts and allantois (data not shown). Absence of vascular tubes was evident at all stages examined, from the onset of cord formation at the 1somite (1S) stage, and throughout the entire time frame of normal tubulogenesis (2S to 6S) (Figure S2E–S2L and data not shown). We examined developmental intermediates at each somite stage (from 1S to 12S, at E8.0–8.5), as well as at E9.0, E9.5 and E10.5. Defects did not result from failed proliferation, as similar numbers of ECs were present in *Rasip1*$^{+/-}$ versus *Rasip1*$^{-/-}$ aortae and we found no proliferation defects (Figure S2M–S2O). Given that failure of tubulogenesis occurred at the onset of vessel formation, prior to the onset of blood flow, and that EC proliferation was not affected, we reasoned that loss of Rasip1 resulted in morphogenetic failure due to cellular defects intrinsic to mutant angioblasts.

## Rasip1 binding partners

While Rasip1 had previously been shown to bind Ras GTPases by *in vitro* pull down assays (Mitin et al., 2004), its physiological binding partners in endothelium and its downstream signaling pathways have remained unknown. To elucidate the molecular mechanism of Rasip1 function during vasculogenesis and lumen formation, we sought to determine its binding partners by two-step affinity purification and mass spectrometry, using a tetracycline inducible stable endothelial cell line (MS1$^{\text{Rasip1-FLAG}}$) (Figure S3A–S3C). Amongst several putative Rasip1 binding partners identified (Figure 2A) were two proteins of particular interest due to their previous implication in vascular development: non-muscle myosin heavy chain IIA (NMHCIIA) and a RhoA-specific GAP, Arhgap29 (Figures S3D and S3E).

NMHCIIA is an important motor protein in the actomyosin complex. NMHCIIA and MLC (myosin light chain) together comprise myosin II, which modulates diverse processes such as cell structure, adhesion, contractility and motility (Conti and Adelstein, 2008; Even-Ram and Yamada, 2007). NMHCIIA often exerts its regulatory control by acting as a scaffold for

signaling molecules, such as kinases and Rho GTPase guanine nucleotide exchange factors (GEFs) (Even-Ram et al., 2007). Recently, it was reported that in VEGF haploinsufficient embryos, NMHCIIA failed to be recruited to the luminal membrane of dorsal aortic ECs, which failed to form vascular lumens (Strilic et al., 2009). NMHCIIA was proposed to regulate actomyosin tension of the cell membrane, driving lumen expansion. In *Rasip1*$^{-/-}$ failed vessels (Figure S4A–S4H) and Rasip1 siRNA depleted cells (Figure S4I–S4L), levels of NMHCIIA at the EC-EC interface appear unchanged, suggesting that recruitment of NMHCIIA to the cell membrane was Rasip1-independent. We therefore reasoned that NMHCIIA activity and function, rather than levels, were likely altered in *Rasip1*$^{-/-}$ mutants.

Arhgap29 (PARG1), the other identified Rasip1 binding partner was known to be expressed in fish vasculature (Gomez et al., 2009) and to possess a GAP domain for RhoA (Myagmar et al., 2005). In mouse embryos, we found that Arhgap29 protein was present in the ECs of the paired aortae during vasculogenesis, in a manner analogous to that reported in fish (Figure 2B). In addition, Rasip1 and Arhgap29 were present together in cytoplasmic punctae in cultured ECs (~50% rate of overlap) (Figure 2C).

## Rasip1 and Arhgap29 are required for *in vitro* lumen formation

Overlap of Rasip1 and Arhgap29 in ECs, both *in vivo* and *in vitro*, suggested that they were likely to function together during blood vessel development. To assess the requirement for Rasip1 and Arhgap29 during *in vitro* tubulogenesis, we used a HUVEC 3D matrix assay that mimics the developmental process of vasculogenesis (Kamei et al., 2006; Sacharidou et al., 2010). To determine whether Rasip1 or Arhgap29 function was required for EC lumen formation *in vitro*, siRNA-depleted cells (Figure 2D and S3F) were assessed for their lumen formation ability. Strikingly, EC lumen formation was completely blocked in siRNA-treated cells (Figure 2E and 2F). Movies of depleted cells showed that although ECs extended cellular processes, these would snap back and rarely maintain connections to the surrounding matrix (Movies S2, S3, S5 and S6). In addition, cells would dynamically make and break contacts with each other, and preliminary lumenal structures within individual ECs initiated but quickly collapsed. In contrast, the control ECs would generate and sustain lumens, maintain steady adherence to the surrounding matrix, and interconnect to form multicellular lumenal structures (Figure 2E, 2F and Movies S1 and S4).

## Rasip1 and Arhgap29 are required for activation of Cdc42 and Rac1 during lumen formation

Previous *in vitro* studies have shown that vascular lumen formation depends on proper regulation of the Rho family of monomeric G proteins (Cdc42/Rac1/RhoA). Specifically, Cdc42 and Rac1 activation were shown to be required for lumen formation in 3D collagen matrix assays, while RhoA activation had the opposite effect and suppressed it (Bayless and Davis, 2002, 2004; Iruela-Arispe and Davis, 2009; Nobes and Hall, 1995; Sacharidou et al., 2010).

We thus examined Rasip1 and Arhgap29 regulation of Rho GTPase activity using this same assay system and found markedly decreased levels of activated Cdc42 and Rac1 levels in siRNA-treated HUVECs (Figure 2G, S3G and data not shown). In addition, we examined a kinase cascade downstream of Cdc42 that was recently shown to be required for *in vitro* EC lumen formation (Koh et al., 2008; Koh et al., 2009). As expected, signaling downstream of Cdc42 and Rac1 were impaired in the absence of Rasip1 or Arhgap29, as the active (phosphorylated) form of key GTPase effector kinases, such as pPak4, pSrc, pB-Raf, pC-Raf and pErk, were reduced in siRNA-depleted ECs (Figure 2H and S3H). Interestingly,

although cell morphology and behavior were similarly affected by absence of either Rasip1 or Arhgap29, some differences in downstream signaling reduction were reproducible (pSrc).

### Rasip1 and Arhgap29 regulate EC architecture via repression of RhoA

In contrast to the reduced activities of Cdc42 and Rac1, we found that RhoA activation was upregulated in the absence of either Rasip1 or Arhgap29 (Figure 2G and S3G). This finding was consistent with the notion that RhoA antagonizes lumen formation and must be kept at bay (Bayless and Davis, 2002). Because activated RhoA was shown to suppress vascular lumen maintenance via cytoskeletal modulation (Bayless and Davis, 2004), we examined the EC cytoskeleton in the absence of either Rasip1 or Arhgap29. Strikingly, individual knockdowns of Rasip1 or Arhgap29 lead to nearly identical defects in EC architecture (Figure 3A–3C). At higher resolution, we observed a significant increase in actin stress fiber assembly (a process dependent on RhoA) in the absence of either Rasip1 or Arhgap29 (Figure 3D–3F). Moreover, we assessed ‘stabilized’ microtubules and found a sharp decrease in acetylated tubulin in Rasip1 or Arhgap29 depleted cells (Figure 3G–3J). This effect was also surprisingly detectable *in vivo* in E9.5 *Rasip1*$^{-/-}$ whole embryo lysates (Figure 3K). Rasip1 and Arhgap29 therefore are both independently required for cellular structure and contractility of ECs.

We next examined possible Rasip1 modulation of myosin II. We reasoned that myosin II activity was likely to be altered, due to four findings: 1. Rasip1 binds both a RhoA-specific GAP (Arhgap29) and NMHCIIA, which is RhoA-dependent (Figure 2A); 2. activated RhoA levels were increased in Rasip1/Arhgap29-depleted cells (Figure 2G); 3. stress fiber assembly (known to be RhoA dependent) was significantly increased in Rasip1/Arhgap29-depleted cells (Figure 3D–3F); and 4. Rasip1/Arhgap29-depleted cells display dramatically decreased acetylated tubulin (Figure 3G–3J) and NMHCIIA is known to suppress tubulin acetylation (Even-Ram et al., 2007). We thus examined Rasip1 and Arhgap29 modulation of RhoA-dependant myosin II via the regulatory molecules Rho-kinase (ROCK) and the ROCK substrate Myosin Light Chain (MLC) (Matsumura, 2005; Rikitake and Liao, 2005). Phosphorylated MLC (pMLC) is required for non-muscle myosin II activity and regulation of the actomyosin complex.

Indeed, we found significantly increased levels of pMYPT (T696) (downstream target of ROCK1/2) and pMLC (T18/S19) in the absence of either Rasip1 or Arhgap29 (Figure 3L and 3M). These data further support the hypothesis that myosin IIA activity, not localization, depends on Rasip1 and Arhgap29. In addition, hyperactivation of ROCK/MLC/myosin IIA, and the manifested cytoskeletal alterations, suggest that an important function of Rasip1/Arhgap29 is to suppress ROCK, MLC and thus non-muscle myosin IIA activity via RhoA, during endothelial morphogenesis.

To confirm whether Rasip1 suppression of RhoA signaling played a role during EC lumen formation, we knocked down expression of RhoA in the background of Rasip1 or Arhgap29 loss-of-function. While siRasip1 and siArhgap29 treated cells were blocked in their ability to form lumens *in vitro* (as shown above), this failure was reversed upon co-expression of dominant negative RhoA (Figure 3N). By contrast, dominant negative Cdc42 or Rac1 constructs (Bayless and Davis, 2002) had no effect. These results were further confirmed with co-siRNA treatments to simultaneously knockdown expression of RhoA and either Rasip1 or Arhgap29 (Figure 3O). Thus while siRhoA alone had no effect on *in vitro* lumen formation, it largely rescued the absence of either Rasip1 or Arhgap29.

### Failure of EC-ECM adhesion *in vitro* in the absence of Rasip1 or Arhgap29

As RhoA and NMHCIIA are both known to regulate cell adhesion, we examined both EC-EC and EC-ECM adhesion in Rasip1/Arhgap29-depleted cells. Flow cytometry indicated neither PECAM nor VE-cadherin levels were altered in the absence of Rasip1 or Arhgap29 (Figure S5A and S5B). In addition, despite irregular borders, relatively normal levels of the adhesion molecules ZO-1, β-catenin and PECAM were found at cell-cell interfaces of Rasip1 or Arhgap29 depleted cells (Figure S5C–S5K), suggesting at least grossly that EC-EC adhesion was not reduced.

By contrast, we found that siRNA-treated ECs exhibited significantly reduced adhesion to several types of ECM (Figure S6A and S6B). To assess the molecular machinery that regulates cell adhesion to ECM, we examined focal adhesions, which are structures essential for adhesion of cells to matrix during both embryonic development and blood vessel formation (Bohnsack and Hirschi, 2003; Goody and Henry, 2010). Focal adhesions first appear as adhesion complexes (FXs), which mature into focal adhesions (FAs) and then into fibrillar adhesions (FBs) (Tomar and Schlaepfer, 2009). An excellent indicator of immature FX is phosphorylated paxillin (pPaxillin), which is recruited to nascent FXs, but lost as they mature (Zaidel-Bar et al., 2007). We found that pPaxillin (Y118) positive FXs were expanded in siRasip1 or siArhgap29 depleted cells compared to control siRNA-treated cells (Figure 4A–4C), especially at the cell periphery (Figure 4D–4F). In addition, total levels of pPaxillin (Y118) were significantly increased in the absence of Rasip1 or Arhgap29, both *in vitro* and *in vivo* (Figure 4G), indicating a likely increase in immature FXs. Of note, it has been reported that in plated cells, FXs are born at the cell periphery and mature into FBs at the center of cell (Tomar and Schlaepfer, 2009), suggesting that in the absence of either Rasip1 or Arhgap29, FX are favored over FAs/FBs and maturation of adhesions is inhibited.

We then assessed mature focal adhesions (FBs), which contain clustered or ‘activated’ integrins, but lack paxillin (Morgan et al., 2009). Given the central role of β1 integrin (β1) in adhesion of ECs to ECM, as well as in blood vessel formation (Drake et al., 1992; Zovein et al., 2010), we examined activated β1 using an ‘activated’ state-specific antibody, 9EG7 (Bazzoni et al., 1995). In the absence of either Rasip1 or Arhgap29, activated β1 integrin levels were reduced 70% and 80% respectively (Figure 4H, black columns). To reveal total cell surface β1 integrin levels, we artificially activated β1 using manganese (Lenter et al., 1993) and found these unchanged (Figure 4H, white columns). These results suggest that Rasip1 is required for activation, rather than levels, of β1 integrin.

We further examined the reduction of activated β1 integrin in Rasip1/Arhgap29 depleted ECs using immunofluorescent staining with 9EG7. Control HUVECs displayed FBs as linear tracts of clustered β1 integrin in the central region of the cell (Figure 4I). By contrast, siRasip1- or siArhgap29-treated cells lacked all FB organization into tracts, showing only reduced and punctate β1 foci (Figure 4J and 4K). This effect was similarly observed in another EC line, MS1 (Figure S6C–S6E). Thus, activated β1 levels and distribution were severely affected in the absence of Rasip1 or Arhgap29, although total β1 remained unchanged (including *in vivo*, Fig. S6F and S6G). Given that failure to disassemble FX is known to block FB formation and β1 activation (Zaidel-Bar et al., 2007), our data suggested that the lack of FB tracts observed in siRNA-treated cells was likely due to a failure of FX disassembly.

To test whether integrin activation specifically required RhoA and/or non-muscle myosin IIA suppression, we attempted to rescue integrin activation with either blebbistatin (non-muscle myosin II inhibitor) (Straight et al., 2003) or Y-27632 (ROCK inhibitor) (Rikitake and Liao, 2005). While both drugs partially rescued β1 integrin activation, neither did so

well, implicating possible integrin redundancy and a requirement for additional signaling pathways (Figure S6H).

We therefore asked whether other integrins, such as β3, might also depend on Rasip1. We examined αvβ3 in siRNA-treated cells by flow cytometry using the antibody LM609 (Byron et al., 2009). A significant decrease in β3 in untreated (Figure S6I, black columns) versus manganese-treated cultures (Figure S6I, white columns) suggested that activated β3 depended on Rasip1/Arhgap29 activity. We thus examined activated αvβ3 integrin using an activated state specific antibody, WOW-1 (Kiosses et al., 2001), and observed a similarly modest but measurable decrease in levels in siRNA-treated cells (data not shown). Similarly, blebbistatin and Y-27632 treatment showed a trend towards rescue, although it was not statistically significant (Figure S6J). These data suggest that Rasip1 and Arhgap29 work together to regulate EC adhesion to the surrounding ECM, likely via β1 and possibly other integrins, and in the absence of either molecule the dynamic maturation of adhesion contacts is compromised, reducing EC-ECM adhesion.

## Rasip1 is required for proper *in vivo* endothelial-ECM adhesion

To validate our *in vitro* findings that Rasip1 regulates EC adhesion, we examined the interface between adjacent embryonic ECs (EC-EC), as well as between ECs and surrounding ECM (EC-ECM), in *Rasip1*$^{+/-}$ and *Rasip1*$^{-/-}$ embryos. Given that tight junctions (TJs) and adherens junctions (AJs) components play critical roles in epithelial lumen formation (Lampugnani et al., 2010), we first examined *in vivo* EC-EC junctions. While claudin-5 and ZO-1 (TJs) highlighted narrow peripheral junctions between wild type aortal ECs at E8.5 (Figure 5A, 5A′, 5C and 5C′), TJs were found in clusters at the center of *Rasip1*$^{-/-}$ cords (Figure 5B, 5B′, 5D and 5D′). Similarly, VE-cadherin (AJs) was normally only at peripheral junctions (Figure 5E and 5E′), however it was ectopically distributed in *Rasip1*$^{-/-}$ cords (Figure 5F and 5F′). E8.5 mutant aortic ECs also remained distinctly cuboidal, similar to β1-depleted ECs (Zovein et al., 2010) (Figure 5C–5F′, and data not shown).

We found the opposite situation when we examined adhesion of ECs to the surrounding matrix. Aortic cords normally undergo tubulogenesis in immediate contact with both collagen IV and fibronectin (FN), which are secreted by the surrounding trunk mesenchyme, as well as laminin secreted by the underlying endoderm. While *Rasip1*$^{-/-}$ aortic ECs remained tightly associated with the endoderm, mutant ECs lost adherence to the surrounding mesoderm (Figure 5D, 5F, 5H, 5L and 5N). This selective failure of EC-ECM adhesion was observed at all stages after 3S during vasculogenesis. At 3S, both wildtype and mutant cord ECs were in contact with mesenchymal cells in a nearly identical manner (Figure 5I and 5J). However, between 4 to 6S, an intervening space progressively expanded (Figure 5K–5N). Indeed, while ECs remained in tight contact with the endoderm, a highly reproducible and growing cavity appeared between the mesenchyme and the *Rasip1*$^{-/-}$ aortic cord ECs. Because of the failure of the aortae to acquire patency, the diameter of these cords was reduced compared to wild type, with most of them under 5 m (Figure 5O). Together, these data suggest the interesting possibility that the overlying mesenchyme provides structural support, via integrins, to the expanding aortic endothelial tubes.

## Rasip1 is required for establishment of endothelial apicobasal polarity

Because junctional proteins were mislocalized along the apical/luminal surface of Rasip1$^{-/-}$ ECs, and because GTPase activity is known to control cell polarity (Etienne-Manneville and Hall, 2002), we asked whether EC apicobasal polarity depended on Rasip1. We first examined expression of recently described endothelial apical molecules, shown to drive vascular lumen formation (Strilic et al., 2009). We found that both CD34 and F-actin

localized normally in *Rasip1*$^{-/-}$ aortic ECs (Figure S7A-S7D). In addition, both moesin and podocalyxin (PODXL) displayed normal localization, being primarily expressed along EC surfaces facing the cord center (apical) in both wild type and *Rasip1*$^{-/-}$ vessels (Figure S7E–S7L).

The presence of TJs in the center of *Rasip1*$^{-/-}$ cords, however, suggested EC polarity defects. We examined initiation of lumen formation in wild type cords and found early clearance of TJs (ZO-1) at the cord center, at 2S (Figure 6A-6A″). Thus, ECs rapidly refine their apicobasal character during lumen formation, with junctional ZO-1 segregating from apical PODXL. In contrast, *Rasip1*$^{-/-}$ cords displayed a distinct failure to clear the apical membrane of TJs as lumen formation initiated (Figure 6B-6B″). This ectopic localization of ZO-1 persisted in mutant cords in older embryos (Figure S7M-S7N″). Aberrant apical localization of the normally junctional ZO-1 molecules was particularly striking upon co-staining with the apical marker PODXL. In wild type ECs, the two quickly segregated during lumen formation, with ZO-1 at the cord periphery and PODXL along internal surfaces (Figure 6C—6C″). However, in *Rasip1*$^{-/-}$ ECs, the two exhibited significant sustained overlap (Figure 6D—6D″). ZO-1 was not only ectopically located on apical, but also basal, EC surfaces. Transmission electron microscopy (TEM) studies also revealed failure of the cord-to-tube transition at early stages of morphogenesis (4S stage), revealing slit-like lumenal spaces and mislocalized cell-cell junctions (Figure 6E, 6F) and confirming that ectopic localization of ZO-1 represents ectopic junctions.

We examined cell polarity in *Rasip1*$^{-/-}$ ECs by assessing the polarity determinant Par3. As EC polarity was recently shown to be disrupted (and Par3 expression reduced) in β1 integrin null ECs (Zovein et al., 2010), we asked whether Par3 expression or localization depends on Rasip1. In wild type aortic ECs, like ZO-1, Par3 was expressed along the entire apical membrane prior to lumen formation, but redistributed junctionally (apicolaterally) as vascular lumens formed (Figure 6G, 6I and 6K). These results were consistent with reports that Par3 localizes to TJs in polarized epithelial cells (Jaffe et al., 2008). In *Rasip1*$^{-/-}$ ECs, by contrast, Par3 initially localized normally to the apical, pre-lumen EC surface, but it subsequently failed to be cleared during lumen formation (Figure 6H, 6J, and 6L). Par3 could be observed, like ZO-1, in clusters between apposed ECs along the apical membrane. Interestingly, occasionally we observed proper TJ localization in Rasip1 null ECs, and in these rare instances lumens formed normally (Figure S7O). However, these isolated lumens were small and formed isolated pockets, but did not connect into functional tubes.

## DISCUSSION

Here, we identify a critical requirement for Rasip1 during normal blood vessel tubulogenesis. We show that Rasip1 together with Arhgap29, a RhoA-specific GAP, suppresses RhoA signaling and dampens ROCK and non-muscle myosin IIA activities in endothelial cells (Figure 7A). When Rasip1 or Arhgap29 are absent, RhoA activation is elevated, resulting in excessive actomyosin contractility, disruption of cell polarity and consequent failure of lumen morphogenesis. Basal adhesion contacts, between ECs and surrounding ECM, fail to mature (as assessed by lack of integrin activation), resulting in disassociation of endothelium from surrounding mesenchyme. Apical adhesion is also disrupted, as junctional contacts are mislocalized within the central portion of cords, blocking the ability of ECs to open coherent lumens (Figure 7B). Inappropriate segregation of apicobasal character is evidenced by sustained overlap of apical and junctional (lateral) markers in *Rasip1*$^{-/-}$ ECs. Additionally, Rasip1/Arhgap29 suppression of RhoA promotes Cdc42 and Rac1 activation, which in turn activates downstream kinases, including Pak4, Src, B-Raf, C-Raf and Erk, required for *in vitro* EC lumen formation (Koh et al., 2008; Koh et al., 2009). Rasip1 thus represents a unique molecular bottleneck, as it integrates Rho

family GTPase signaling to control cell polarity and adhesion, thereby coordinating endothelial morphogenesis and blood vessel tubulogenesis.

## Rasip is required for endothelial cell polarity

Three key points led us to expect defective cell polarity in *Rasip1* null angioblasts. First, Rasip1 regulates endothelial GTPase activity. Second, decades of classical work have demonstrated regulation of cell polarity by Rho GTPases, such as Cdc42 (Etienne-Manneville and Hall, 2002). Finally, recent findings pointed to the importance of proper cell polarity during vascular lumen formation, both in early embryonic vessels, as well as those formed later during embryogenesis (Strilic et al., 2009; Zovein et al., 2010).

It was therefore surprising to observe no changes in subcellular localization or levels of CD34, F-actin, moesin or podocalyxin in *Rasip1* null cord ECs, as these molecules are localized to the apical EC surface and are required for lumen formation. However, disruption of cell polarity in *Rasip1* null cord ECs was indeed revealed by junctional protein mislocalization. Significant overlap of apical podocalyxin with ZO-1 in Rasip1 null ECs, and ectopic VE-cadherin, at multiple points along the apical surface and at all stages examined (both early and late), showed that the apical membrane did not properly segregate from the lateral/junctional membrane. Moreover, basal EC character was also compromised, as ectopic ZO-1 and VE-cadherin were found along basal membranes and functional integrin adhesion to the surrounding matrix was severely reduced.

Cell polarity defects in *Rasip1* null cord ECs were further revealed by mislocalization of the polarity determinant Par3. Indeed, in the absence of Rasip1, we found a clear failure of Par3 to segregate normally to cell-cell junctions, away from the apical membrane. Par3 is known to associate with the aPKC polarity complex in epithelial cells (Suzuki and Ohno, 2006) and to be important in establishment of arterial cell polarity (Zovein et al., 2010). We note that while Par3 was previously found to be localized basally in older arterial vessels and reduced in the absence of β1 integrin (Zovein et al., 2010), localization of Par3 in early angioblasts of the dorsal aortae was clearly junctional, and levels appeared unchanged in *Rasip1* null ECs. It is conceivable that vasculogenic vessels form differently from angiogenic vessels formed later, but that key signaling molecules are nonetheless conserved.

We note that between clusters of junctional molecules (ZO-1/Par3/VE-cadherin), we observed slit-like openings, in which apical molecules like podocalyxin/moesin were expressed normally. We speculate that much of the lumen formation molecular pathway actually occurs ‘normally’ in the absence of Rasip1, albeit discontinuously. In Rasip1 null ECs, TJ/AJ localization likely occurs stochastically, such that the morphogenetic process is short-circuited, blocking functional lumen formation and tubulogenesis.

## Rasip regulation of cell adhesion to ECM via maturation of adhesion contacts

The primary defect observed in ECs in the absence of Rasip1 function is failure of proper EC adhesion regulation, both between cells and with surrounding matrix. Failure of adhesion to matrix was evident both in live cell imaging of *in vitro* EC lumen formation in siRasip1-treated cells, as well as in sections of *Rasip1*$^{-/-}$ lumenless aortic cords. This EC-ECM failure was particularly striking in collagen 3D cultures, as ECs extended processes that transiently adhered to the surrounding matrix as they initiated lumen formation, but snapped back and collapsed repeatedly as they lost traction. These behavioral effects can be explained by impaired focal adhesion maturation in Rasip1-depleted cells. Whether resulting immature focal adhesions are merely weaker, or whether outside-in or inside-out signaling via focal adhesion components is compromised, can not be distinguishable from these studies. It will be interesting to identify additional Rasip1 binding partners, as it can

complex with number Rho and Ras family GTPases (Mitin et al., 2004), and further dissect signaling pathways and their effects on cell adhesion and architecture.

An interesting point regarding maturation of endothelial adhesion contacts is that Rasip1 appears to promote engagement of multiple integrins. Specifically, decrease of both β1 and αvβ3 in siRasip1-depleted cells, suggests other integrins are likely similarly regulated. Lumen dependence on multiple integrins is supported by antibody-based knockdowns targeting β1 (Drake et al., 1992) or αvβ3 (Drake et al., 1995), which blocked lumen formation in chick aortae. Redundancy of integrin dependence on Rasip1 during lumen formation likely explains the more profoundly compromised vascular phenotype observed in *Rasip1*$^{-/-}$ mice versus EC-specific deletions of single integrins, which have not shown global lumen failure (Carlson et al., 2008; Tanjore et al., 2008). In *Rasip1*$^{-/-}$ aortae, we suggest all required integrins have been blocked, as Rasip1 controls their activation. One relevant study bypassed the issue of integrin redundancy by examining fibronectin (FN) null embryos, as FN is a common ligand for a number of integrins, including β1 and αvβ3 (George et al., 1997). Interestingly, the endocardial lumen was absent in *FN*$^{-/-}$ embryos, and aortic ECs partially detached from surrounding mesenchyme, similar to Rasip1 null embryos. However, *Rasip1*$^{-/-}$ do not phenocopy *FN*$^{-/-}$ embryos, likely because other matrix components are also required. Together, these data suggest that Rasip1 is critical to integrin function in ECs.

## Diverse cellular mechanisms drive vascular lumen formation?

An unexpected finding in our studies involved the growing gap between the trunk mesenchyme and the lumenless *Rasip1*$^{-/-}$ aortic cords. Our data suggests that Rasip1-deficient aortic ECs are unable to maintain proper integrin-mediated adhesion to the surrounding mesenchymal ECM and imply that the mesenchyme actively provides support during lumen expansion. We note that while this gap is pronounced surrounding the mutant aortic cords, similar gaps around other vessels are variable or absent, such as those in the yolk sac. It is therefore possible that different blood vessels create lumens by different cellular mechanisms, but common molecular mechanisms.

Indeed other biological ‘tubes’ often depend on multiple spatially- and/or temporally-specific mechanisms for lumen formation. The Drosophila trachea, for instance, ranges from intracellular vacuole-based lumen generation in fine terminal cells, to multicellular budding and lumen expansion in primary tracheal branches (Lubarsky and Krasnow, 2003). Therefore, although we present here a mechanism for lumen formation based on angioblast adhesion regulation, we predict that the highly complex and heterogeneous developing vascular system (Aird, 2007) will exhibit regional differences with respect to the cellular mechanisms employed to generate lumens.

Indeed, controversy has emerged in the field of vascular biology regarding how vascular lumens form. Some observations, both *in vitro* and *in vivo*, have suggested that lumen formation occurs via intracellular vacuoles, which emerge and fuse (Davis and Bayless, 2003; Kamei et al., 2006). While other observations have favored a mechanism based on angioblast cords rearranging their junctions to the periphery and opening up a central lumen based on active cytoskeletal forces (Jin et al., 2005; Strilic et al., 2009). Our *in vivo* observations of murine aortic ECs reveal no evidence for vacuole fusion, similar to (Strilic et al., 2009). However, cultured ECs in 3D matrices clearly exhibit vacuole fusion (seen in Movies S1–S3). Of great interest then is that failure of lumen formation in both systems occurs in the absence of Rasip1. This places Rasip1 in a critical regulatory position over the molecular machinery that controls cellular processes, such as the cell polarity, cytoskeleton (i.e. cell shape), and localization or robustness of cell junctions and adhesion contacts.

Future studies will be aimed at identifying commonalities and differences in different EC types.

### Rasip1 regulation of GTPase signaling

Our data suggests that Rasip1 suppresses RhoA (known to inhibit lumen formation) and promotes activation of Cdc42 and Rac1 (both known positively mediate lumen formation). Rescue experiments demonstrate that failure of tubulogenesis in the absence of either Rasip1, or its effector Arhgap29, can be fully restored by dominant negative RhoA or siRhoA treatment.

As a consequence, we have focused on Rasip1 regulation of RhoA signaling. However, the sharp decrease in Cdc42 and Rac1 activity in the absence of Rasip1 is of particular interest, as these GTPases play direct roles in assembly and disassembly of junctional components, as well as cytoarchitecture such as filopodia formation (Popoff and Geny, 2009). Indeed, we see decreased filopodia in the absence of Rasip1 function (data not shown). In addition, Cdc42 has been directly linked to maintenance of EC-EC junctions via VE-cadherin (Broman et al., 2006), as well as vacuole-based lumen formation (Bayless and Davis, 2002). However, we identified no relevant effectors for Cdc42 or Rac1 as binding partners in our mass spectrometry screen, therefore it is possible that their regulation by Rasip1 is indirect and occurs via the RhoA pathway.

### Critical role of actomyosin contractility for vascular tubulogenesis

One likely critical effector of vascular tubulogenesis is the RhoA-specific GAP and Rasip1 binding partner Arhgap29, which suppresses RhoA signaling specifically in developing blood vessels. Finding that Rasip1 also bound NMHCIIA, which is regulated by RhoA, raises the distinct possibility that a key role of Rasip1 is to suppress actomyosin contractility via suppression of RhoA. This is an appealing model, as angioblasts must dramatically change their shape during lumen formation, transforming from an initially rounded cuboidal morphology, to an exceedingly flattened one. Increased intracellular contractility would inhibit such a shape change. The recent report that NMHCIIA recruitment to the luminal surface of ECs was defective in the lumenless cords of VEGF heterozygotes (Strilic et al., 2009) adds another interesting dimension to the role of contractility during lumen formation. In this case, lack of contractility fails to ‘bend’ the luminal membrane and ‘open up’ the central lumen. Together, the data suggests that precisely controlled levels of myosin II activity, and contractility, are required for vascular lumens: too much contractility (as in *Rasip1*$^{-/-}$ ECs) or too little contractility (as in *VEGF*$^{+/-}$ ECs) both lead to lumen failure.

### Conclusions

Rasip1 therefore acts as a unique, endothelial-specific, integration node for Rho GTPase signaling, controlling EC morphogenesis from cord-to-patent blood vessel via cell polarity and adhesion regulation. Given that most approaches to anti-angiogenic therapies have focused on targeting extrinsic growth factors, such as VEGF, rather than cell intrinsic effects, future studies of Rasip1 and the molecular circuitry under its control, hold great promise to provide novel tools and models for furthering clinical therapies.

## EXPERIMENTAL PROCEDURES

### Generation of *Rasip1* null allele

The mouse 129sv genomic DNAs (provided by UTSW transgenic core) were used as template for the generation of a conditionally null allele by amplifying a region of DNA flanking exon 3 and two additional homologous arms 5′ and 3′ using Takara’s LA Taq polymerase. The three subclones were cloned into a neomycin/thymidine kinase double

selection vector pGKneo-TK2-Floxed-Flip (kindly provided by Thomas Carroll). The exon 3 containing subclone was inserted into a multiple cloning site flanked by loxP sites. Neomycin resistance cassette was designed being flanked by Flp recombinase target (FRT) sites for removing if necessary. This targeting vector was electroporated into mouse embryonic stem cells by UTSW transgenic core. 5′ and 3′ external probes for Southern blot screening were PCR amplified and subcloned into pGEM-T-Easy vector (Invitrogen). SphI digested purified genomic DNA from each clones was screened by Southern blot using both probes for homologous recombination. The correct clone was injected into C57BL6/J blastocysts for generating Rasip1 targeted mouse line. After germ line transmission confirmation, the animals were bred with Sox2-Cre mice (kindly provided by Thomas Carroll) to generate a Rasip1 null allele. Litters were genotyped by PCR using primers listed in the Supplemental Experimental Procedures. The wild type, floxed, and null alleles give bands of 165 base pairs, 247 base pairs, and 331 base pairs, respectively.

### Embryo Histology and in situ Hybridization

Mouse, frog and zebrafish in situs and mouse beta-galactosidase staining were performed as previously described (Neumann et al., 2009; Xu et al., 2009a). All cloning primers are listed in the Supplemental Experimental Procedures. Connexin40 (Gja5) clone was obtained from Open Biosystems (MMM1013-9202306).

### Cell Culture

Human umbilical vein ECs (HUVEC, PCS100-010) and mouse pancreatic islet EC line MILE SVEN 1 (MS1, CRL-2279) were obtained from ATCC (or Lonza) and cultured per ATCC's standard protocols. 293AD cells (kindly provided by Eric Olson) were grown in Dulbecco's Modified Eagle Medium (DMEM, GIBCO) with 10% Fetal Bovine Serum (FBS).

### Establishment of MS1$^{Rasip1-FLAG}$ cell line

C-terminal FLAG tagged Rasip1 cassette was inserted into pEN_TTmiRc2 and then sub-cloned into pSLIK-Neo (kindly provided by Zhijian Chen) by gateway cloning. 10μg Rasip1-FLAG expressing pSLIK vector was transfected into 293AD cells together with 7.5μg of each of the two packaging plasmids pLp1, and pLp2, and 5μg of the vesicular stomatitis virus (VSV) G envelope plasmid pLp-VSVG diluted in Opti-MEM (Invitrogen). The medium was changed 12 hours post-transfection, and the viral particles were harvested and filtered through 45 micron micro filters upon applying to MS1 ECs for infection. The infected MS1 cells were selected with 4mg/ml G418 (Sigma), and the expression of Rasip1-FLAG were analyzed by western blot and immunofluorescent staining using a monoclonal anti-M2 antibody (Sigma).

### Tandem Affinity Purification of Rasip1 Complex

MS1$^{Rasip1-FLAG}$ cells were cultured with the presence of 1μg/ml doxycyclin for 3 days to induce the expression of exogenous Rasip1-FLAG fusion protein. The cell lysate from ten 10cm dishes were incubated with 50μl Anti-FLAG M2 Affinity Gel (Sigma A2220) as per Sigma's standard protocol. The bound proteins were eluted with 200μl 0.2mg/ml FLAG peptide (Sigma F3290). The elutes were then incubated with 5μg Rasip1 antibody (Abcam ab21018) or IgG agarose (Sigma A0919, for control) at 4C for 1 hour. The Rasip1 antibody bound protein complex were then incubated with 50μl rec-Protein G Sepharose 4B (Zymed 10–1241) at 4C for 1 hour, followed by elution with 40μl 0.1mg/ml human RASIP1 immunizing peptide (aa951-962, UTSW Peptide Synthesis Core Facility). The final elutes were resolved by SDS-PAGE and processed by silver staining using Invitrogen's

SilverQuest kit (LC6070). Specific bands were cut off and subjected to Mass Spectrometry as previously published (Xu et al., 2009b).

### siRNA Transfection

siRNAs obtained from IdtDNA, Invitrogen, and Dharmacon were transfected into cultured endothelial cells using standard protocol as previously described (Koh et al., 2008). Sequences of siRNAs are listed Supplemental Experimental Procedures.

### Immunofluorescent Staining

Immunufluorescent staining in tissues was performed as per standard protocol previously published (Villasenor et al., 2008). Antibodies used in this study can be found in Supplemental Experimental Procedures.

### *In vitro* lumen formation and pull-down assays

HUVEC lumen and tube formation in 3D collagen matrices were performed as previously described (Koh et al., 2009).

### TEM

Carried out by UTSW Electron Microscopy Core Facility as per their standard protocols.

### Flow Cytometry

HUVECs detached from the dish by 50mM EDTA (pH8.0) treatment were washed with and resuspended as $10^7$/ml in labeling buffer ($Ca^{2+}$ free PBS containing 0.5% BSA). After incubation at 37C for 15 min with or without 5mM $MnCl_2$, the cells were labeled with primary antibodies at 1:50 for 30 min on ice. Cells were then washed twice and labeled with fluorophore conjugated secondary antibody in labeling buffer at 4C for 30 min. After final wash (twice in chilled PBS), cells were resuspended in 500μl 1% PFA and subjected to FACS analysis (UTSW Flow Cytometry Facility). Blebbistatin and Y-27632 were kindly provided by Helen Yin.

### Microscopy, Imaging and Statistical Analysis for *in vitro* Lumen Formation

Visualization and image acquisition of EC lumen formation was performed using an inverted microscope (CKX41: Olympus) and real time-lapse imaging of ECs undergoing lumen and tube formation was done using a Nikon TE2000-E system with a temperature-controlled chamber. Image analysis was performed using MetaMorph software. Statistical analysis of EC vasculogenesis was performed using SPSS 11.0 software. Statistical significances were assessed by a paired-samples *t test*.

## Supplementary Material

Refer to Web version on PubMed Central for supplementary material.

## Acknowledgments

We thank Thomas Carroll for gene targeting instructions, knockout vector and antibodies. We also thank Janet Rossant and Eli Keshet for the Flk1-EGFP/lacZ mice; Mark Henkemeyer for the EphB4-LacZ mice; Sanford Shattil for the WOW-1 antibody; James Amatruda for assistance with zebrafish; and Jose Cabrera for help with figures. We thank the UTSW Core Facilities: Imaging, Transgenic, Peptide Synthesis and TEM cores for assistance. We thank Natalia Mitin, Eric Olson, Jenny Hsieh, Paul Krieg, Michelle Tallquist and Mike Buszczak for critical reading of the manuscript, and Natalia Mitin, Thomas Carroll and the CCLARTB group for essential discussions. This work is supported by NIH Predoctoral training grant GM007062 (BS), AHA Predoctoral fellowship 09PRE2070035 (KX), NIH HL59373 (GED) and NIH DK079862, AHA Grant-in-Aid 0755054Y and the Basil O'Connor March of Dimes Award (OC).

## References


Aird WC. Phenotypic heterogeneity of the endothelium: II. Representative vascular beds. Circ Res. 2007; 100:174–190. [PubMed: 17272819]

Andrew DJ, Ewald AJ. Morphogenesis of epithelial tubes: Insights into tube formation, elongation, and elaboration. Dev Biol. 341:34–55. [PubMed: 19778532]

Bayless KJ, Davis GE. The Cdc42 and Rac1 GTPases are required for capillary lumen formation in three-dimensional extracellular matrices. J Cell Sci. 2002; 115:1123–1136. [PubMed: 11884513]

Bayless KJ, Davis GE. Microtubule depolymerization rapidly collapses capillary tube networks in vitro and angiogenic vessels in vivo through the small GTPase Rho. J Biol Chem. 2004; 279:11686–11695. [PubMed: 14699132]

Bazzoni G, Shih DT, Buck CA, Hemler ME. Monoclonal antibody 9EG7 defines a novel beta 1 integrin epitope induced by soluble ligand and manganese, but inhibited by calcium. J Biol Chem. 1995; 270:25570–25577. [PubMed: 7592728]

Bergers G, Hanahan D. Modes of resistance to anti-angiogenic therapy. Nat Rev Cancer. 2008; 8:592–603. [PubMed: 18650835]

Bohnsack BL, Hirschi KK. The FAKs about blood vessel assembly. Circ Res. 2003; 92:255–257. [PubMed: 12595334]

Broman MT, Kouklis P, Gao X, Ramchandran R, Neamu RF, Minshall RD, Malik AB. Cdc42 regulates adherens junction stability and endothelial permeability by inducing alpha-catenin interaction with the vascular endothelial cadherin complex. Circ Res. 2006; 98:73–80. [PubMed: 16322481]

Byron A, Humphries JD, Askari JA, Craig SE, Mould AP, Humphries MJ. Anti-integrin monoclonal antibodies. J Cell Sci. 2009; 122:4009–4011. [PubMed: 19910492]

Carlson TR, Hu H, Braren R, Kim YH, Wang RA. Cell-autonomous requirement for beta1 integrin in endothelial cell adhesion, migration and survival during angiogenesis in mice. Development. 2008; 135:2193–2202. [PubMed: 18480158]

Carmeliet P, Lampugnani MG, Moons L, Breviario F, Compernolle V, Bono F, Balconi G, Spagnuolo R, Oosthuyse B, Dewerchin M, et al. Targeted deficiency or cytosolic truncation of the VE-cadherin gene in mice impairs VEGF-mediated endothelial survival and angiogenesis. Cell. 1999; 98:147–157. [PubMed: 10428027]

Connolly JO, Simpson N, Hewlett L, Hall A. Rac regulates endothelial morphogenesis and capillary assembly. Mol Biol Cell. 2002; 13:2474–2485. [PubMed: 12134084]

Conti MA, Adelstein RS. Nonmuscle myosin II moves in new directions. J Cell Sci. 2008; 121:11–18. [PubMed: 18096687]

Davis GE, Bayless KJ. An integrin and Rho GTPase-dependent pinocytic vacuole mechanism controls capillary lumen formation in collagen and fibrin matrices. Microcirculation. 2003; 10:27–44. [PubMed: 12610662]

Davis GE, Koh W, Stratman AN. Mechanisms controlling human endothelial lumen formation and tube assembly in three-dimensional extracellular matrices. Birth Defects Res C Embryo Today. 2007; 81:270–285. [PubMed: 18228260]

Drake CJ, Cheresh DA, Little CD. An antagonist of integrin alpha v beta 3 prevents maturation of blood vessels during embryonic neovascularization. J Cell Sci. 1995; 108(Pt 7):2655–2661. [PubMed: 7593306]

Drake CJ, Davis LA, Little CD. Antibodies to beta 1-integrins cause alterations of aortic vasculogenesis, in vivo. Dev Dyn. 1992; 193:83–91. [PubMed: 1540708]

Etienne-Manneville S, Hall A. Rho GTPases in cell biology. Nature. 2002; 420:629–635. [PubMed: 12478284]

Even-Ram S, Doyle AD, Conti MA, Matsumoto K, Adelstein RS, Yamada KM. Myosin IIA regulates cell motility and actomyosin-microtubule crosstalk. Nature cell biology. 2007; 9:299–309.

Even-Ram S, Yamada KM. Of mice and men: Relevance of cellular and molecular characterizations of myosin IIA to MYH9-related human disease. Cell Adh Migr. 2007; 1:152–155. [PubMed: 19262128]

George EL, Baldwin HS, Hynes RO. Fibronectins are essential for heart and blood vessel morphogenesis but are dispensable for initial specification of precursor cells. Blood. 1997; 90:3073–3081. [PubMed: 9376588]

Gomez GA, Veldman MB, Zhao Y, Burgess S, Lin S. Discovery and characterization of novel vascular and hematopoietic genes downstream of etsrp in zebrafish. PLoS One. 2009; 4:e4994. [PubMed: 19308258]

Goody MF, Henry CA. Dynamic interactions between cells and their extracellular matrix mediate embryonic development. Molecular reproduction and development. 2010; 77:475–488. [PubMed: 20108219]

Iruela-Arispe ML, Davis GE. Cellular and molecular mechanisms of vascular lumen formation. Dev Cell. 2009; 16:222–231. [PubMed: 19217424]

Jaffe AB, Kaji N, Durgan J, Hall A. Cdc42 controls spindle orientation to position the apical surface during epithelial morphogenesis. J Cell Biol. 2008; 183:625–633. [PubMed: 19001128]

Jin SW, Beis D, Mitchell T, Chen JN, Stainier DY. Cellular and molecular analyses of vascular tube and lumen formation in zebrafish. Development. 2005; 132:5199–5209. [PubMed: 16251212]

Kamei M, Saunders WB, Bayless KJ, Dye L, Davis GE, Weinstein BM. Endothelial tubes assemble from intracellular vacuoles in vivo. Nature. 2006; 442:453–456. [PubMed: 16799567]

Kiosses WB, Shattil SJ, Pampori N, Schwartz MA. Rac recruits high-affinity integrin alphavbeta3 to lamellipodia in endothelial cell migration. Nat Cell Biol. 2001; 3:316–320. [PubMed: 11231584]

Koh W, Mahan RD, Davis GE. Cdc42- and Rac1-mediated endothelial lumen formation requires Pak2, Pak4 and Par3, and PKC-dependent signaling. J Cell Sci. 2008; 121:989–1001. [PubMed: 18319301]

Koh W, Sachidanandam K, Stratman AN, Sacharidou A, Mayo AM, Murphy EA, Cheresh DA, Davis GE. Formation of endothelial lumens requires a coordinated PKCepsilon-, Src-, Pak- and Raf-kinase-dependent signaling cascade downstream of Cdc42 activation. J Cell Sci. 2009; 122:1812–1822. [PubMed: 19435802]

Kucera T, Eglinger J, Strilic B, Lammert E. Vascular lumen formation from a cell biological perspective. Novartis Foundation symposium. 2007; 283:46–56. discussion 56–60, 238–241. [PubMed: 18300413]

Lampugnani MG, Orsenigo F, Rudini N, Maddaluno L, Boulday G, Chapon F, Dejana E. CCM1 regulates vascular-lumen organization by inducing endothelial polarity. J Cell Sci. 2010; 123:1073–1080. [PubMed: 20332120]

le Noble F, Moyon D, Pardanaud L, Yuan L, Djonov V, Matthijsen R, Breant C, Fleury V, Eichmann A. Flow regulates arterial-venous differentiation in the chick embryo yolk sac. Development. 2004; 131:361–375. [PubMed: 14681188]

Lenter M, Uhlig H, Hamann A, Jeno P, Imhof B, Vestweber D. A monoclonal antibody against an activation epitope on mouse integrin chain beta 1 blocks adhesion of lymphocytes to the endothelial integrin alpha 6 beta 1. Proc Natl Acad Sci U S A. 1993; 90:9051–9055. [PubMed: 7692444]

Lubarsky B, Krasnow MA. Tube morphogenesis: making and shaping biological tubes. Cell. 2003; 112:19–28. [PubMed: 12526790]

Matsumura F. Regulation of myosin II during cytokinesis in higher eukaryotes. Trends in cell biology. 2005; 15:371–377. [PubMed: 15935670]

Mitin NY, Ramocki MB, Zullo AJ, Der CJ, Konieczny SF, Taparowsky EJ. Identification and characterization of rain, a novel Ras-interacting protein with a unique subcellular localization. J Biol Chem. 2004; 279:22353–22361. [PubMed: 15031288]

Morgan MR, Byron A, Humphries MJ, Bass MD. Giving off mixed signals--distinct functions of alpha5beta1 and alphavbeta3 integrins in regulating cell behaviour. IUBMB Life. 2009; 61:731–738. [PubMed: 19514020]

Myagmar BE, Umikawa M, Asato T, Taira K, Oshiro M, Hino A, Takei K, Uezato H, Kariya K. PARG1, a protein-tyrosine phosphatase-associated RhoGAP, as a putative Rap2 effector. Biochem Biophys Res Commun. 2005; 329:1046–1052. [PubMed: 15752761]

Neumann JC, Dovey JS, Chandler GL, Carbajal L, Amatruda JF. Identification of a heritable model of testicular germ cell tumor in the zebrafish. Zebrafish. 2009; 6:319–327. [PubMed: 20047465]

Nobes CD, Hall A. Rho, rac and cdc42 GTPases: regulators of actin structures, cell adhesion and motility. Biochem Soc Trans. 1995; 23:456–459. [PubMed: 8566347]

O'Brien LE, Zegers MM, Mostov KE. Opinion: Building epithelial architecture: insights from three-dimensional culture models. Nat Rev Mol Cell Biol. 2002; 3:531–537. [PubMed: 12094219]

Popoff MR, Geny B. Multifaceted role of Rho, Rac, Cdc42 and Ras in intercellular junctions, lessons from toxins. Biochimica et biophysica acta. 2009; 1788:797–812. [PubMed: 19366594]

Reardon DA, Desjardins A, Rich JN, Vredenburgh JJ. The emerging role of anti-angiogenic therapy for malignant glioma. Curr Treat Options Oncol. 2008; 9:1–22. [PubMed: 18256938]

Rikitake Y, Liao JK. ROCKs as therapeutic targets in cardiovascular diseases. Expert Rev Cardiovasc Ther. 2005; 3:441–451. [PubMed: 15889972]

Sacharidou A, Koh W, Stratman AN, Mayo AM, Fisher KE, Davis GE. Endothelial lumen signaling complexes control 3D matrix-specific tubulogenesis through interdependent Cdc42- and MT1-MMP-mediated events. Blood. 2010

Shalaby F, Rossant J, Yamaguchi TP, Gertsenstein M, Wu XF, Breitman ML, Schuh AC. Failure of blood-island formation and vasculogenesis in Flk-1-deficient mice. Nature. 1995; 376:62–66. [PubMed: 7596435]

Siemann DW, Bibby MC, Dark GG, Dicker AP, Eskens FA, Horsman MR, Marme D, Lorusso PM. Differentiation and definition of vascular-targeted therapies. Clin Cancer Res. 2005; 11:416–420. [PubMed: 15701823]

Straight AF, Cheung A, Limouze J, Chen I, Westwood NJ, Sellers JR, Mitchison TJ. Dissecting temporal and spatial control of cytokinesis with a myosin II Inhibitor. Science. 2003; 299:1743–1747. [PubMed: 12637748]

Strilic B, Kucera T, Eglinger J, Hughes MR, McNagny KM, Tsukita S, Dejana E, Ferrara N, Lammert E. The molecular basis of vascular lumen formation in the developing mouse aorta. Dev Cell. 2009; 17:505–515. [PubMed: 19853564]

Suzuki A, Ohno S. The PAR-aPKC system: lessons in polarity. J Cell Sci. 2006; 119:979–987. [PubMed: 16525119]

Tanjore H, Zeisberg EM, Gerami-Naini B, Kalluri R. Beta1 integrin expression on endothelial cells is required for angiogenesis but not for vasculogenesis. Dev Dyn. 2008; 237:75–82. [PubMed: 18058911]

Tomar A, Schlaepfer DD. Focal adhesion kinase: switching between GAPs and GEFs in the regulation of cell motility. Current opinion in cell biology. 2009; 21:676–683. [PubMed: 19525103]

Villasenor A, Chong DC, Cleaver O. Biphasic Ngn3 expression in the developing pancreas. Dev Dyn. 2008; 237:3270–3279. [PubMed: 18924236]

Wang HU, Chen ZF, Anderson DJ. Molecular distinction and angiogenic interaction between embryonic arteries and veins revealed by ephrin-B2 and its receptor Eph-B4. Cell. 1998; 93:741–753. [PubMed: 9630219]

Xu K, Chong DC, Rankin SA, Zorn AM, Cleaver O. Rasip1 is required for endothelial cell motility, angiogenesis and vessel formation. Dev Biol. 2009a

Xu M, Skaug B, Zeng W, Chen ZJ. A ubiquitin replacement strategy in human cells reveals distinct mechanisms of IKK activation by TNFalpha and IL-1beta. Mol Cell. 2009b; 36:302–314. [PubMed: 19854138]

Zaidel-Bar R, Milo R, Kam Z, Geiger B. A paxillin tyrosine phosphorylation switch regulates the assembly and form of cell-matrix adhesions. J Cell Sci. 2007; 120:137–148. [PubMed: 17164291]

Zovein AC, Luque A, Turlo KA, Hofmann JJ, Yee KM, Becker MS, Fassler R, Mellman I, Lane TF, Iruela-Arispe ML. Beta1 integrin establishes endothelial cell polarity and arteriolar lumen formation via a Par3-dependent mechanism. Dev Cell. 2010; 18:39–51. [PubMed: 20152176]

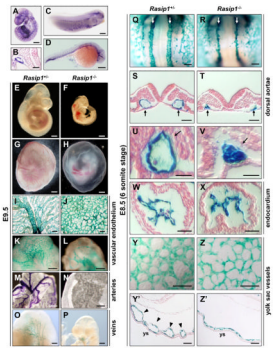

**Figure 1. *Rasip1* is essential for vascular tubulogenesis in all blood vessels**

(**A–D**) Rasip1 expression is conserved in the embryonic vasculature across species shown by *in situ* hybridization; mouse (**A**, E9.5; **B**, E8.5 transverse section, left dorsal aorta), *Xenopus tropicalis* (**C**, st.30), and zebrafish (**D**, 24hpf). (**E–H**) E9.5 littermate mouse embryos showing defects in *Rasip1*$^{-/-}$ embryos (**F**) and yolk sacs (**H**). (**I–L**) Whole mount Flk1-lacZ beta-galactosidase staining of *Rasip1*$^{+/-}$ (**I, K**) and *Rasip1*$^{-/-}$ (**J, L**) yolk sacs (**I, J**) and embryonic heads (**K, L**), showing narrow *Rasip1*$^{-/-}$ blood vessels that fail to remodel. (**M–P**) Connexin40 (Cx40 or Gja5) (**M, N**) or EphB4-lacZ (**O, P**) in littermate E9.5 *Rasip1*$^{+/-}$ and *Rasip1*$^{-/-}$ yolk sacs (**M, N**) or embryos (**O, P**) showing failed arterial (**M, N**) and venous (**O, P**) differentiation in *Rasip1*$^{-/-}$ vessels. (**Q–Z′**) Flk1-LacZ beta-galactosidase staining of littermate E8.5 (6 somite stage) *Rasip1*$^{+/-}$ and *Rasip1*$^{-/-}$ embryos and tissues, in whole mount or section. (**Q, R**) Ventral views of E8.5 embryonic paired dorsal aortae. Anterior is up. (**S–V**) Transverse sections of E8.5 embryos, through the trunk region, posterior to the heart. (**U, V**) Closeup views, showing open lumens in *Rasip1*$^{+/-}$*;Flk1-lacZ* embryos (**S, U**), but lumenless cords in *Rasip1*$^{-/-}$*;Flk1-lacZ* embryos (**T, V**). Sections through hearts of E8.5 (**W, X**), showing absence of a lumen in the endocardium of *Rasip1*$^{-/-}$*;Flk1-lacZ* embryos (**X**). Yolk sacs in whole mount (**Y, Z**) or section views (**Y′, Z′**). Vascular tubes are absent in all *Rasip1*$^{-/-}$ vessels examined. Arrows, dorsal aortae. Arrowheads, yolk sac vessels. ys: yolk sac. Scale bars: 500μm (**A, E–H**), 250μm (**C**), 200μm (**K–P**), 100μm (**D, I, J, Q, R, Y, Z**), 50μm (**B, S–Z, Y′, Z′**). See also Figures S1 and S2.

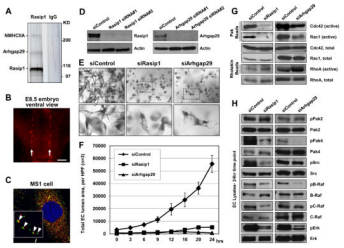

**Figure 2. Rasip1 and Arhgap29 are required for *in vitro* EC lumen formation and regulation of small GTPase signaling**

(**A**) Silver staining of the affinity-purified Rasip1 complex. Marked bands were identified by mass spectrometry. (**B**) Arhgap29 protein in E8.5 mouse embryonic aortic ECs, ventral view. Arrows, paired dorsal aortae. Scale bar: 50μm. (**C**) Rasip1 and Arhgap29 expression in cultured EC (MS1). Arrowheads, Rasip1/Arhgap29 co-localization in punctae. Nuclei, DAPI (blue). (**D**) Western blots of Rasip1 and Arhgap29 following siRNA treatment of cultured HUVECs in 3D collagen matrices. (**E**) Lumen formation is blocked in siRasip1-/siArhgap29-treated HUVECs cultured in 3D collagen matrices. Arrowheads, visible EC lumen. (**F**) Quantification of lumen formation in control- or siRasip1-/siAhgap29- treated HUVECs. (**G**) Cdc42, Rac1 and RhoA activities and (**H**) reduction of kinase signaling downstream of Cdc42/Rac1 pathway in siRNA-treated HUVECs in 3D cultures at 24hrs. Error bars represent standard deviation. See also Figure S3.

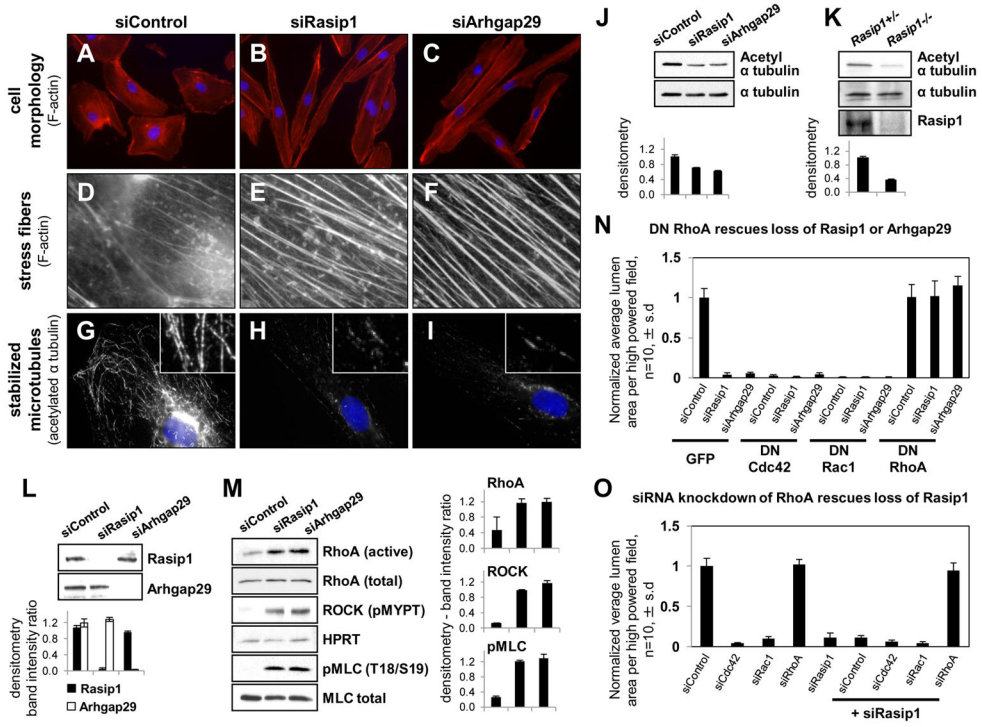


**Figure 3. Rasip1 and Arhgap29 regulate EC architecture and tubulogenesis through Rho family GTPases**

(**A–F**) Immunofluorescent phalloidin staining showing gross cell morphology and stress fibers in siRNA-treated HUVECs. (**G–I**) 'Stabilized' microtubule shown by acetylated α-tubulin staining in siRNA-treated HUVECs. Insets, high magnification view of microtubules. Nuclei, DAPI (blue). (**J, K**) Acetylated α–tubulin level is down regulated in siRNA treated ECs *in vitro* (**J**) and *in vivo* in E9.5 *Rasip1*$^{-/-}$ embryos (**K**), n = 2. (**L, M**) Western blots showing RhoA and ROCK activity (pMYPT, T696), phosphorylation of myosin light chain (pMLC, T18/S19) in siRNA-treated HUVECs, n = 3. (**N**) Dominant negative (DN) RhoA rescues *in vitro* lumenless phenotype in 3D collagen matrices in siRasip1-/siArhgap29-treated HUVECs. (**O**) Loss of Rasip1, which causes a lumenless EC phenotype in 3D collagen matrices, is rescued by siRNA knockdown of RhoA. Error bars represent standard deviation. See also Figure S4.

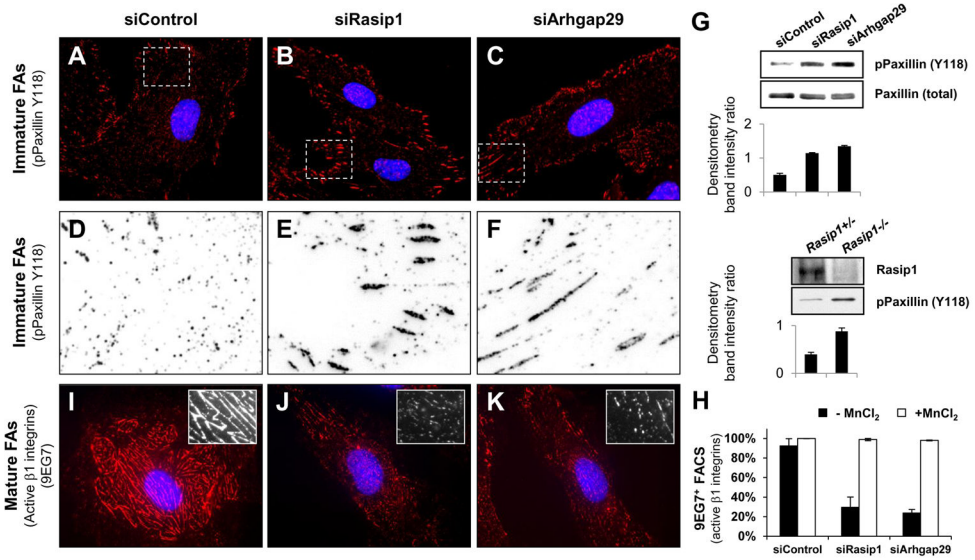


**Figure 4. Rasip1 and Arhgap29 are required for maturation of endothelial-ECM adhesion**

(**A–F**) Immature focal adhesions shown by phosphorylated Paxillin (Y118) staining in siRNA-treated HUVECs. (**G**) Phosphorylated Paxillin (Y118) is up regulated in siRNA treated ECs *in vitro* and *in vivo* in *Rasip1*$^{-/-}$ embryos, n = 2. (**H**) Flow cytometry showing decrease in activated β1 integrin (9EG7) in the absence of Rasip1 or Arhgap29. $MnCl_2$ (5mM) treatment reveals total surface levels of integrins are unchanged. (**I–K**) Mature fibrillar adhesions shown by activated β1 integrin (9EG7) expression in siRNA-treated HUVECs. Insets, high magnification view of 9EG7$^{+}$ FBs. Nuclei, DAPI (blue). Error bars represent standard deviation. See also Figures S5 and S6.

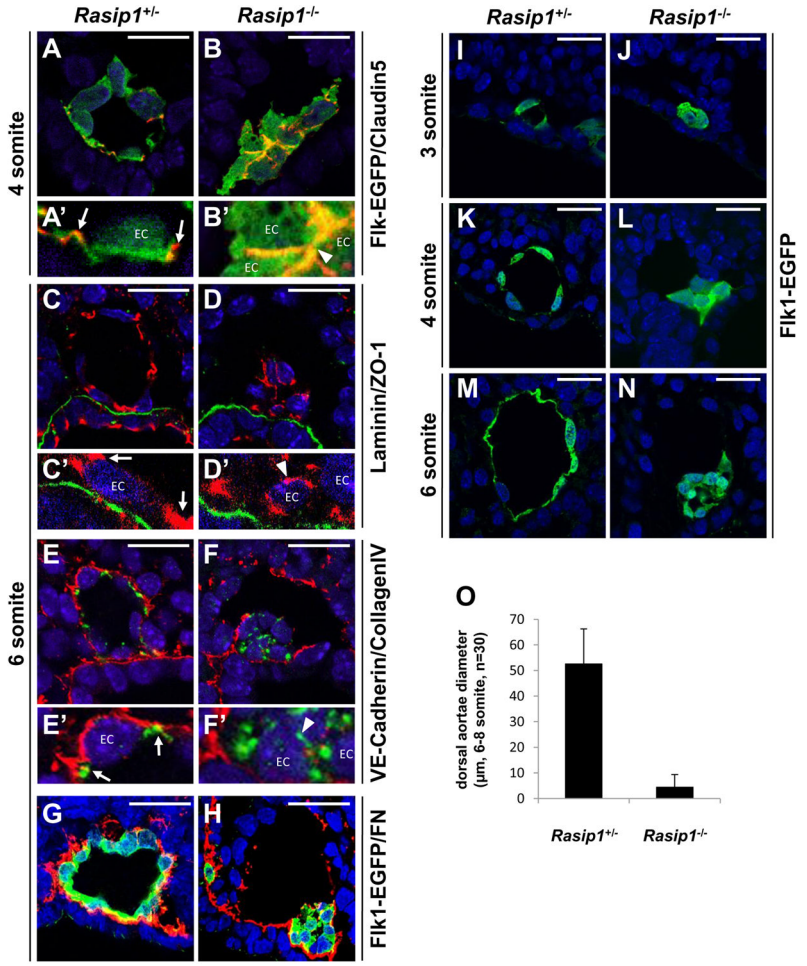


**Figure 5. *Rasip1*$^{-/-}$ angioblasts remain cuboidal and fail to adhere to surrounding ECM**

**(A–N)** Confocal immunofluorescence microscopy of 3–6 somite *Rasip1*$^{+/-}$ (**A, C, E, G, I, K, M**) and *Rasip1*$^{-/-}$ (**B, D, F, H, J, L, N**) dorsal aortae (Flk1-EGFP, **A, B, G, H, IN**) in transverse sections: (**A, B**) claudin-5, (**C, D**) ZO-1 and laminin, (**E, F**) VE-cadherin and collagen IV, and (**G, H**) fibronectin. Nuclei, DAPI (blue). (**O**) Average dorsal aortae diameter at 6–8 somite stage, n=30. Arrows, EC-EC junctions in *Rasip1*$^{+/-}$ embryos. Arrowheads, mislocalized EC-EC junctions. Scale bars, 25 μm. Error bars represent standard deviation.

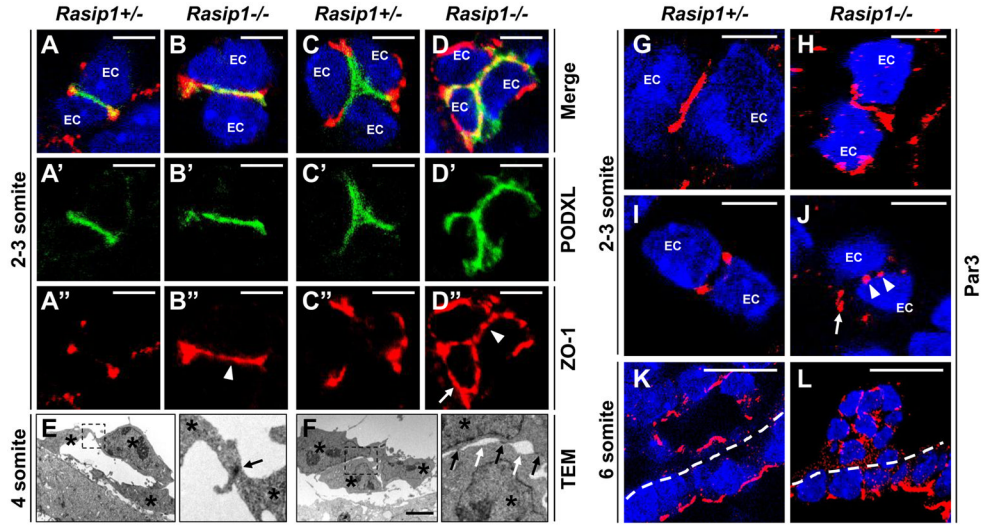


**Figure 6. *Rasip1*$^{-/-}$ angioblasts display defective cell polarity and fail to localize junctional proteins to cord periphery**

**(A–D, G–L)** Confocal immunofluorescence microscopy of *Rasip1*$^{+/-}$ (**A, C, G, I, K**) and *Rasip1*$^{-/-}$ (**B, D, H, J, L**) aortic ECs in transverse sections: podocalyxin (green), ZO-1 (red), and Par3 (**G–L,** red). Nuclei, DAPI (blue). (**E, F**) *Rasip1* null aortic cord angioblasts display mislocalized EC-EC TJs. TEM images of transverse sections of *Rasip1*$^{+/-}$ (**E**) and *Rasip1*$^{-/-}$ (**F**) littermates, at 4-somite stage. (**E, F**) Black arrows, tight junctions; white arrows, slits/isolated lumens between ECs. (**A″, D″, J**) Arrows, ectopic basal TJs; arrowheads, ectopic apical TJs; dotted line, basal endoderm surface. Scale bars, 5 μm (**A–J**), 20μm(**K, L**). See also Figure S7.

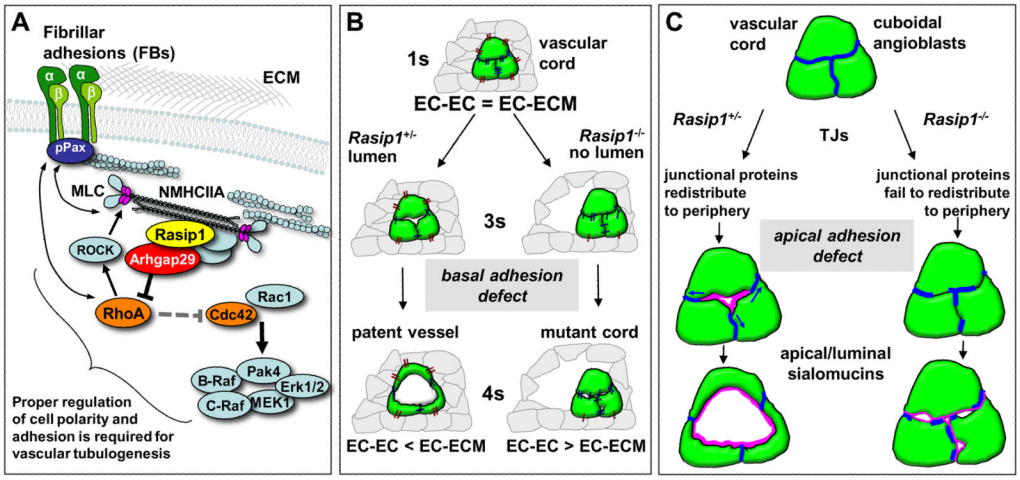


**Figure 7. Models of Rasip1 regulation of embryonic vascular tubulogenesis**

(**A**) Rasip1 regulates EC contractility and adhesion by modulating Rho family small GTPases. (**B, C**) The balance between EC-EC and EC-ECM adhesion is critical to vascular cord to tube transition. (**B**) Loss of integrin adhesion at the basal cell surface and (**C**) failure of junctional protein redistribution from the apical cell surface to the cord periphery result in failed vascular tubulogenesis.